Chapter 4
Development of High-Throughput Screening Device for Neurodegenerative Diseases

Tsuneo Urisu, Zhi-hong Wang, Hidetaka Uno, Yasutaka Nagaoka, Kei Kobayashi, Miho Goto-Saitoh, Yoshinori Suzuki and Yoko Urabe

Abstract Neurodegenerative diseases such as amyotrophic lateral sclerosis and Alzheimer's disease are intractable diseases, for which neither the cause nor treatment method are known in spite of more than 100 years of research. The reason for this is (1) it is not easy to sample neurons, the affected parts, during the lifetime of the patients and (2) there have never been suitable and precise high-throughput methods for analyzing the function of the neuron network. The first problem is now being solved by iPS technologies. We are now developing several technologies to solve the second problem. The problem of low seal resistance, the weak point of the incubation-type planar patch clamp (by which we can measure the ion-channel current from the neuron network at many measuring points), was overcome by using a salt-bridge Ag/AgCl electrode. The ion-channel current from the neuron network was measured for the first time by a planar patch clamp using this stable electrode. A new type of substrate for the planar patch clamp was developed, and a high density but spatially homogeneous neuron network was successfully formed. By combining these device technologies and the human iPS technology, we are now developing a disease model for neurodegenerative diseases.

Keywords Neurodegenerative disease · High-throughput screening · Neuron network · Planar patch clamp · Ion-channel · iPS

4.1 Introduction

Neurodegenerative diseases such as Alzheimer's disease (AD) and amyotrophic lateral sclerosis (ALS) are intractable diseases for which neither the cause nor reliable treatment methods have been established. The reason why these diseases

T. Urisu (✉) · Z. Wang · H. Uno · Y. Nagaoka · K. Kobayashi · M. Goto-Saitoh · Y. Suzuki · Y. Urabe
Institute of Innovation for Future Society, Nagoya University, Furo-Cho, Chikusaku, Nagoya 464-8603, Japan
e-mail: t.urisu@nanobio.nagoya-u.ac.jp

J. Sone and S. Tsuji (eds.), *Intelligent Nanosystems for Energy, Information and Biological Technologies*, DOI 10.1007/978-4-431-56429-4_4

are so intractable is (1) it is not easy to sample neurons, the affected parts, during the lifetime of the patients and (2) suitable methods for analyzing the function of the neuron network have never been developed. Animal models are generally used to solve the former problem. Unfortunately, however, the medicine developed using animal models is not so effective for human diseases especially neurodegenerative diseases. This is because animals do not suffer from the same neurodegenerative diseases as humans. Recently developed iPS technology is expected to solve this problem. To apply iPS technology to elucidate the cause and/or the novel drug developments of neurodegenerative diseases, the second problem must be solved. Since many and various kinds of ion-channels are the most important parts that realize signal transduction in the neuron network, the measurement of ion-channel current, which contains information about the release of the neurotransmitter molecules at synapses, is considered to be the most useful method for analyzing neuron network function. The pipette patch clamp is the most excellent standard method of ion-channel current measurements. It is, however, not suitable for multi-point measurement, which is necessary in high-throughput screening applications. Therefore, we must first develop a multi-point measurement method for ion-channel current in the neuron network. Furthermore, neurons easily gather and form aggregations through migrations. The formation method of a spatially homogeneous neuron network suitable for long-term incubation must also be developed. We have developed an incubation-type planar patch clamp [1] and recently succeeded in measuring the spontaneous ion-channel current for the first time by using the planar patch clamp in the neuron network of the cerebral cortex of an embryonic rat with gestational day 17 [2]. We have also succeeded in forming the neuron network with good spatial homogeneity. In this chapter, these results are introduced, and the future prospect of high-throughput screening applications using a human disease model chip is discussed.

4.2 Incubation-Type Planar Patch Clamp

It is expected that the weak point of the pipette patch clamp would be overcome by planarization of the device. For the planar ion-channel biosensor, glass [3], Si [4–6], quartz [7], and a silicon elastomer PDMS (polydimethylsiloxane) [8], etc. have been reported as substrate materials. For Si, it has been considered that the background noise current is large due to the free charge carrier density in the substrate. However, we have recently demonstrated that the noise current can be significantly reduced by using a silicon-on-insulator (SOI) substrate [9]. Since commercialized planar patch clamp devices, however, are not equipped with the incubation function, they cannot be used for a system that requires long incubation periods. New functional analysis and/or screening devices could be realized by adding an incubation function, such as an extra-cellular matrix (ECM) coating on the substrate surface to the conventional planar patch clamp method, and these would be especially useful in applications such as in vitro systems of neurons and neuron

networks using dissociated cultured neurons [10–13]. Moreover, the planar patch clamp method enables simultaneous measurement of multi-point ion-channel currents and advanced 2-D bio-imaging. We have developed an incubation-type planar patch clamp device and demonstrated its operation using TRPV1-expressing human embryonic kidney (HEK) 293 cells and capsaicin as a ligand molecule [1, 2, 14]. In this experiment, we have used SOI substrates as the sensor chip material. But the chip fabrication process using diamond drilling followed by focused ion beam for micropore formation was not necessarily suitable for expanding to the multi-point measurement, which was necessary for high-throughput screening applications. The recently developed light-gated ion-channel method is extremely suitable for the investigation of neural cell and/or neuron network functional analysis due to its excellent time and space resolutions [15, 16]. We also think that this noble technology is useful for the performance test of ion-channel biosensors.

In this work, we have newly developed a biosensor chip fabrication process suitable for multi-point measurements using plastic materials, such as polymethylmethacrylate (PMMA) and polycarbonate (PC) substrates, using several advanced photolithographic microfabrication techniques followed by electroforming, ultra-precision machining, hot embossing, and focussed ion beam process. Plastic materials have excellent characteristics as sensor chip material. Noise due to parasitic capacitance is sufficiently low due to their low dielectric constant. Several nano-microstructures can be easily formed by advanced microfabrication techniques. In this work, the ion-channel biosensor with incubation function was constructed using a PMMA or PC sensor chip, and excellent performance equivalent to the pipette patch clamp was confirmed by using a channelrhodopsin (ChR)-wide receiver (ChRWR), which was the light-gated ion-channel developed by Wang et al. [17].

4.2.1 Fabrication of Biosensor Chip

4.2.1.1 Hot Embossing and Metal Mould

The fabrication process using plastic materials and the structure of the sensor chip are shown in Fig. 4.1. The basic structure of the sensor chip was formed by double-sided hot embossing using a machine made by Engineering System Co., Ltd. The brass mould (mould 2 in Fig. 4.1) for forming the pipette solution wells (a in Fig. 4.1) was fabricated by ultra-precision machining equipment, Robonano (FANUC Ltd.). The scanning electron microscopy (SEM) image of the square pillar structure on the brass mould (mould 2) is shown in Fig. 4.1. The thickness of the thin film structure (b in Fig. 4.1) was controlled with good reproducibility by selecting the thickness of the original PMMA or PC substrate, usually 0.2 mm, and the height of the square pillar structure (193 $\pm$ 2 μm). Temperature control of the moulds was important to form a good quality thin film structure for the sensor chip at the pipette solution well. The temperature conditions were investigated using the

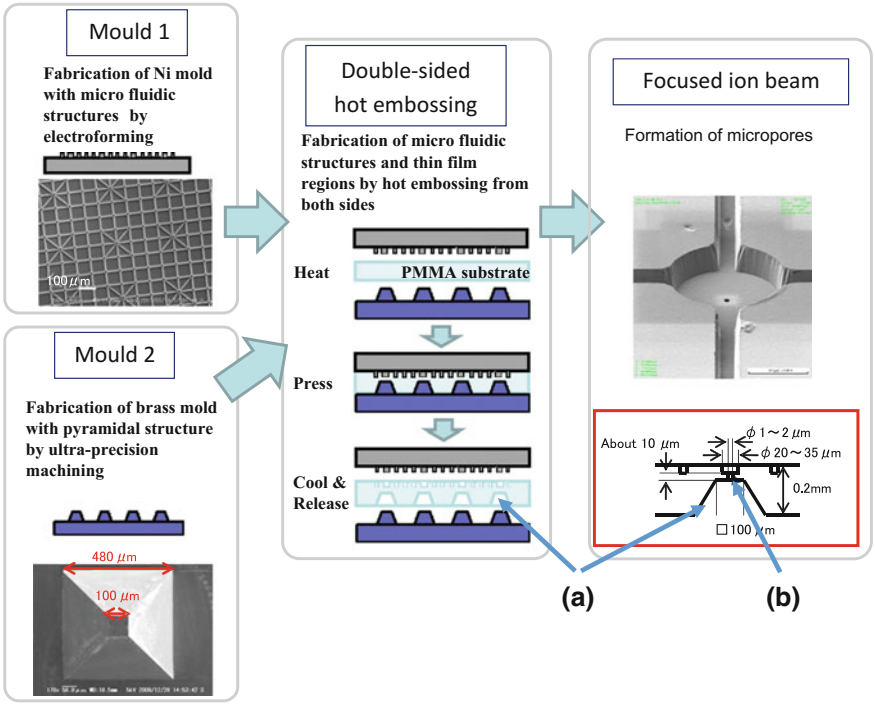

Fig. 4.1 Schematic drawing of fabrication protocol of planar patch clamp substrate by hot embossing. *a* Pipette solution well. *b* Thin film structure

mirror-polished Si wafer as the upper mould. The typical embossing conditions used in the case of PMMA were: upper and lower mould temperatures of 180 and 140 °C, respectively, loading pressure limit of 3500 N, lowering speed of the upper mould 10 μm/s, pressing time of 60 s, and cooling speed of 0.5 °C/s. Mould 1 in Fig. 4.1, which has a lattice pattern on the surface, was used in this work to form the substrate for the HEK293 cells. The lattice pattern forms the microfluidic structure on the substrate surface by embossing. The round areas formed at the crossing points of the lattice pattern of the upper mould were effective to fix the position of the cell. This Ni upper mould was fabricated by electroforming (IKEX Industry Co., Ltd.), for which the master mould was formed by photolithography using positive resist (AZ P4903, AZ Electronic Materials) on the one-side-mirror-polished Si(100) substrate. The electroforming was carried out after forming a thin Ni film on the surface of the resist pattern by sputtering. The Ni mould precisely replicates the resist pattern within the preciseness of the optical microscopy evaluations. It is noted that the side wall of the resist pattern was declined by about 20° from the vertical by baking at 120 °C for 90 min after the development. The upper side mould was aligned to the lower side mould so that the round area for the cell trapping on the upper side mould came into the square

pattern to form the pipette solution well [18]. The structure of the substrate for the neuron network formation is described in Sect. 4.4.

4.2.1.2 Formation of Micropore by Focussed Ion Beam (FIB)

The micropore with diameter of 1.5–2 μm was formed by focused ion beam (FIB) machine (Seiko Instruments Ltd.) at almost the centre of the round area on the pipette solution well. The ion-channel current was measured through this micropore. In the case of the plastic substrate, a Cu thin film was deposited on the surface of both sides of the substrate to reduce the charge-up effects during the FIB processing. This Cu thin film was removed using diluted HNO_3 solution after the micropore formation. The acceleration voltage and the current of the Ga ion beam were 30 keV and 50 pA.

4.2.2 Device Structure of Ion-Channel Biosensor

Figure 4.2a shows the schematic structure of the ion-channel biosensor used in this work. A photograph of the actual device is shown in Fig. 4.2b. The sensor chip was sandwiched between the upper (bath solution side) and the lower (pipette solution side) polydimethylsiloxane (PDMS) plates. Microfluidic circuits were formed inside the lower PDMS plate to supply and exhaust the pipette solutions. The bath solutions were supplied or exhausted through polytetrafluoroethylene (PTFE) tubes (not shown). The weak point of the incubation-type planar patch clamp is the low-seal resistance (Rj in Fig. 4.3a). In the pipette patch clamp, seal resistance larger than 1 GΩ is usually obtained; however, in the case of the incubation-type planar patch clamp, the seal resistance is easily decreased by more than two orders of magnitude due to the extra cellular matrix coated on the sensor chip surface, which makes the gap between the cell membrane and the sensor chip surface larger. Thus, as can easily be understood from Fig. 4.3a, fluctuation of the interface potential between the electrolyte solution and the Ag/AgCl electrode surface causes

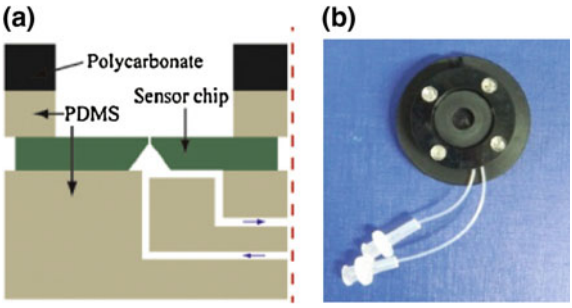

Fig. 4.2 **a** Schematic drawing of planar patch clamp ion-channel biosensor and **b** top view of the device

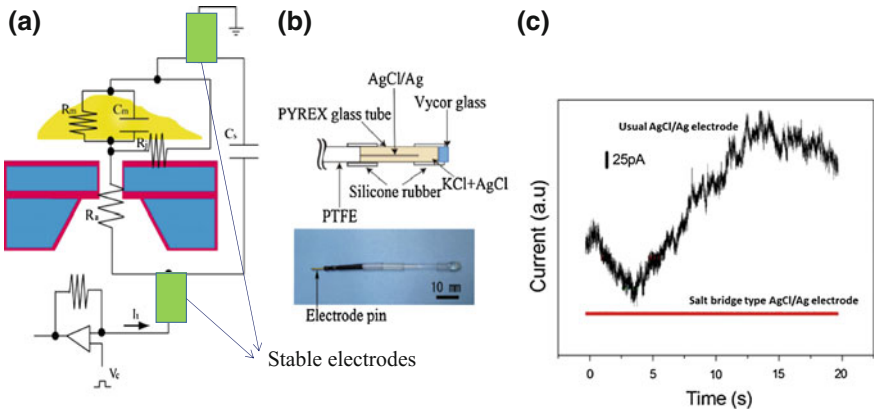

Fig. 4.3 **a** Equivalent electric circuit of incubation-type planar patch clamp, **b** structure of salt-bridge stable electrode, and **c** example of noise reduction data by using stable electrode

a large fluctuation in the base line. The stable electrodes of the salt-bridge structure (Fig. 4.3b) were used both for the bath solution side as a ground and the pipette solution side as the membrane voltage electrode [2]. The Ag/AgCl wire of the stable electrode, which was formed by painting the surface of the Ag wire (0.3 mm diameter) with AgCl ink (BAS Inc.), was inserted into a Pyrex glass tube filled with a saturated KCl and AgCl solution, and the tip was sealed with Vycor glass (Gikenkagaku Co. Ltd.). The Ag/AgCl wire was connected to a gold-plated electrode pin, as shown in Fig. 4.3b. The significant reduction in the noise by using the stable electrode is shown by the red line in Fig. 4.3c as an example.

4.2.3 Expression of ChRWR and TRPV1 on HEK293

Channelrhodopsin is also useful when investigating the performance of the ion-channel biosensor. ChRWR is the name given to the chimeric molecule ChR (ABCDEfg) in Ref. [17], and its plasmid construction is reported in detail in the same Ref. [17]. The HEK293 cells, which were a generous gift from Minoru Wakamori of Tohoku University, were cultured at 37 °C and with 5 % CO_2 in Dulbecco's modified eagle's medium (DMEM) (Sigma-Aldrich Co.) supplemented with 10 % fetal bovine serum (FBS, Biological Industries Ltd.) and transfected using Effectene transfection reagent (Qiagen, Tokyo, Japan) in accordance with the manufacturer's instructions. After cloning twice with the addition of G418 (Gibco) in a 10 cm dish, single colonies with bright Venus fluorescence [19, 20] were selected by using a cloning cylinder IWAKITE-32 (Asahi Glass Co., Ltd.) and cultured in a medium containing G418 until they were confluent in the dish. The TRPV1-expressing HEK293 was a gift from Professor Makoto Tominaga of the

Okazaki Institute for Integrative Bioscience. Details of the transfection procedure are reported in Ref. [21].

4.2.4 Culture of HEK293 Cells in Biosensor

The surfaces of both the sensor chips (Si and PMMA in this case) were coated with ECMs of poly-L-lysine (PLL, Sigma-Aldrich Co.), which showed better performance in the preliminary experiments on the culture in the biosensor than the fibronectin used in our previous experiments [1, 14]. The 50 µl solution (0.005 %) was dropped onto the substrate surface followed by incubation for 1–2 days at room temperature. At this stage, the surface density of the ECM was about 3–5 µg/cm^2. After removal of excess solution, the substrate was rinsed with sterilized water, dried under a gentle nitrogen stream, and kept sterile until use. Cells were cultured in dishes filled with the medium under the conventional incubating conditions, i.e., 37 °C and 5 % CO_2. The culture medium was supplemented with Dulbecco's modified eagle medium (DMEM) to which 10 % (v/v) fetal bovine serum (FBS), 1 % (v/v) Glutamax™ (Gibco), and 0.5 % (v/v) penicillin/streptomycin (Gibco) were added. After cells were detached from the culture dishes, the cell suspension was seeded at a density of 100–300 cells/mm^2 on the ECM-coated chip. The channel current was measured after 5 days of culturing, at which point about 70 % confluence was reached in the case of the no cell trapping pattern, as shown in Fig. 4.4a. In the case of the chip with cell trapping pattern, the

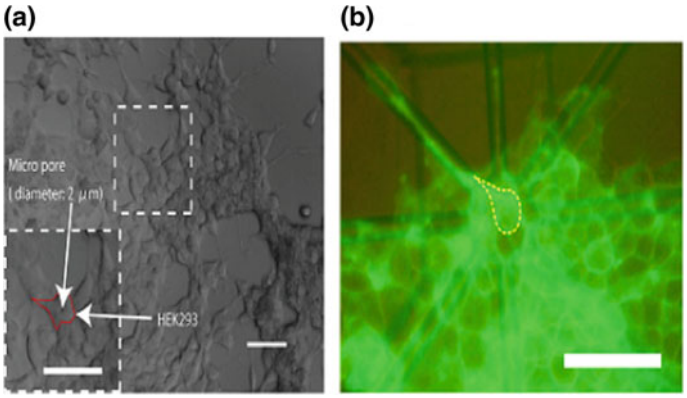

Fig. 4.4 Optical microscopy image of ChRWR expressing HEK293 cells incubated on substrate of incubation-type planar patch clamp biosensor. **a** Bright field image of cells after 5 days incubation on non-patterned substrate. The expanded figure with the cell on the micropore is inserted and **b** fluorescence microscopy image of cells after 3 days incubation on substrate with cell trapping pattern. The cell trapping pattern and the trapped cell is shown by *dotted lines*. The *scale bar* is 50 µm

channel current was measured after about 3 days of culturing when the monolayer colony around the micropore was formed (Fig. 4.4b).

4.2.5 Measurement of Ion-Channel Current

An ion-channel biosensor and preamplifier head stage were set inside the aluminium electromagnetic shield box. The culture medium was replaced with bath and pipette solutions for the upper and lower chambers, respectively. The bath solution in the upper chamber contained: 140 mM NaCl, 3 mM KCl, 10 mM 4-(2-hydroxyethyl)-1-piperazineethanesulfonic acid (HEPES), 2.5 mM $CaCl_2$, 1.25 mM $MgCl_2$, and 10 mM glucose at pH 7.4 (with HCl). The lower chamber solution (pipette solution) contained: 40 mM CsCl, 80 mM $CsCH_3SO_4$, 1 mM $MgCl_2$, 10 mM HEPES, 2.5 mM MgATP, and 0.2 mM Na_2EGTA (pH 7.4) All data were recorded using a patch-clamp amplifier (Axopatch 200B) at room temperature. Data were obtained using a 1 or 2 kHz low-pass filter and output gain of 1 mV/pA, and they were analyzed using pClamp 9.2 software. For whole-cell current recordings, sub-nanometre conductive pores through the cell membrane, which electrically connected the inside of the cell to the lower chamber, were formed by applying the nystatin (Sigma) solution to the lower chamber [22]. The nystatin stock solution was prepared by dissolving nystatin in 1 ml of methanol and successively adding 45 μl of HCl (1 M) and 45 μl of NaOH (1 M), which was then diluted with the lower chamber solution to final concentrations of 100–200 μg/ml before use. The formation of the whole-cell arrangement was confirmed by the observation of a capacitance increase of about 10 pF from 5 to 10 min after the addition of the nystatin solution to the lower chamber.

In the case of the laser-evoked channel current measurements, the laser beam from a semiconductor laser with a 473 nm peak wavelength and 3.2 mW maximum output power (Sumitomo Osaka Cement Co., Ltd) was guided by optical fibre and focused with a microlens with a 26.5 mm focal length under the fluorescence microscope's objective lens (Olympus). The beam diameter at the focal point was 30–100 μm.

4.2.6 Detection of Capsaicin by TRPV1-Expressing HEK293 Biosensor

The ion-channel biosensor could be used in diverse applications ranging from the detection of biological warfare agents to high-throughput screening devices for pharmaceutical development because of its extremely high selectivity and sensitivity. In this work, we constructed a single-channel biosensor shown in Fig. 4.1 using a Si or PMMA sensor chip. First, we constructed the ion-channel biosensor

using TRPV1-expressing HEK293 cells for the detection of capsaicin, which is the main pungent ingredient in hot chili peppers and elicits a sensation of burning pain by selectively activating sensory neurons. Capsaicin stimulation opens the TRPV1 ion-channel, and the non-selective cation flow through the channel is induced. If Ca^{2+} is contained in the extracellular solution, TRPV1 becomes insensitive to capsaicin with prolonged exposure. The mechanism underlying these phenomena is still not clearly understood [21]. The increase in intracellular Ca^{2+} mediates the desensitization, and various signalling pathways are implicated in the desensitization of TRPV1 [21, 23].

To investigate sensitivity for capsaicin, we measured the channel current for the bath solution of several different capsaicin concentrations with draining the bath solution by using a syringe pump (KD Scientific Inc.) at a pumping speed of 12 ml/h. The measurements were carried out at room temperature. The unique inward current followed by desensitization was observed when Ca^{2+} ions were present in the bath solution (Fig. 4.5a). The desensitization was not observed with the Ca^{2+}-free bath solution, as shown in Fig. 4.5a, which agrees well with the reported data measured using a pipette patch clamp [21]. The observed dependence

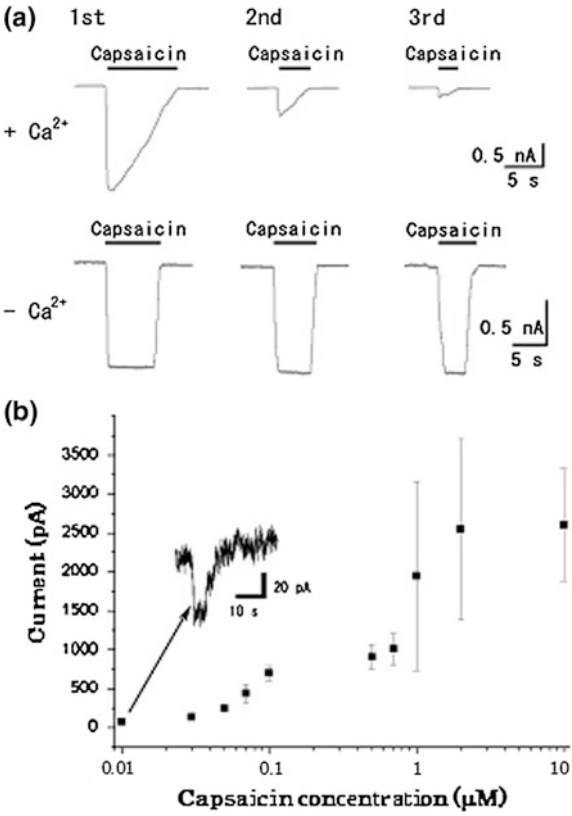

Fig. 4.5 Capsaicin stimulated ion-channel current of TRPV1 expressing HEK293 cells measured by incubation-type planar patch clamp biosensor after 5 days incubation. **a** Current recordings using bath solution containing Ca^{2+} ion (*upper trace*) and not containing Ca^{2+} ion (*lower trace*). **b** Dependence of current on capsaicin concentration. Sensitivity limit is about 10 nM, which is almost equivalent to pipette patch clamp biosensor

of the peak current on the capsaicin concentration is shown in Fig. 4.5b. The lower detection limit was about 0.01 μM. Highly sensitive detection of neurotransmitter molecules and biologically active molecules by the ion-channel biosensor using a pipette patch clamp have been reported [24–26]. In those studies, the noise level including the baseline fluctuations was 5–20 pA (p-p). The noise level of 10–20 pA (p-p) in the present case (Fig. 4.5b) shows that an ion-channel biosensor with almost equivalent performance to the pipette patch clamp can be constructed by using an incubation-type planar patch clamp equipped with a salt-bridge stable electrode, so long as it is the whole-cell mode. In this experiment, use of a stable electrode is essential. The success probability of the device fabrication (number of devices that operated/total number of devices fabricated) was increased from 1 to 2 % (simple Ag/AgCl electrode) to about 60 % (stable electrode).

4.2.7 Laser-Evoked Channel Current Using ChRWR-Expressing HEK293 Cells and Comparison Between Si and PMMA Sensor Chips

The performance of the ion-channel biosensor using a PMMA sensor chip was evaluated by measuring the laser-evoked channel current using ChRWR-expressing HEK293 cells. 20 μl of cell suspension (1×10^4 cells/ml) was injected around the cell trapping area and incubated for 3 days. After confirmation of the formation of a single monolayer colony covering the micropore region (Fig. 4.4b), nystatin solution (100–200 μg/ml) was mixed into the pipette solution, and the formation of the whole-cell mode was easily confirmed by the capacitance increase of about 10 pF caused by the nystatin perforation. After 3 days of incubation, the seal resistance was 7.4 MΩ, and it increased to 9.4 MΩ when negative pressure (∼10 kPa) was applied to the pipette solution side. We also carried out control experiments. No channel currents were observed for cells without ChRWR expression. The dependence of the channel current profiles on the membrane potentials when ChRWR-expressing HEK293 cells were irradiated by a laser (λ = 473 nm, output power = 1.5 mW) driven by rectangular pulses is shown in Fig. 4.6. Similar channel current profiles were observed with the Si sensor chip. In this case, the cell trapping pattern was formed on the Si chip surface by photolithography using SU8 negative resist [27]. Channel current profiles in the case of the PMMA sensor chip agree well with the reported profile (ABCDEfg in Fig. 6A of Ref. [17]) measured using the pipette patch clamp, for the important points: almost no desensitization in the current profile, relatively sharp *on* profile (∼10 ms), and slower *off* profile (∼20 ms).

Much work has been done on the molecular mechanisms relating to the *on* and *off* profile of the channel current induced by the photo-excitation of channelrhodopsin [17, 28–30]. There are, however, still many unclear points. Widely accepted arguments about the mechanisms of photoexcitation and the following

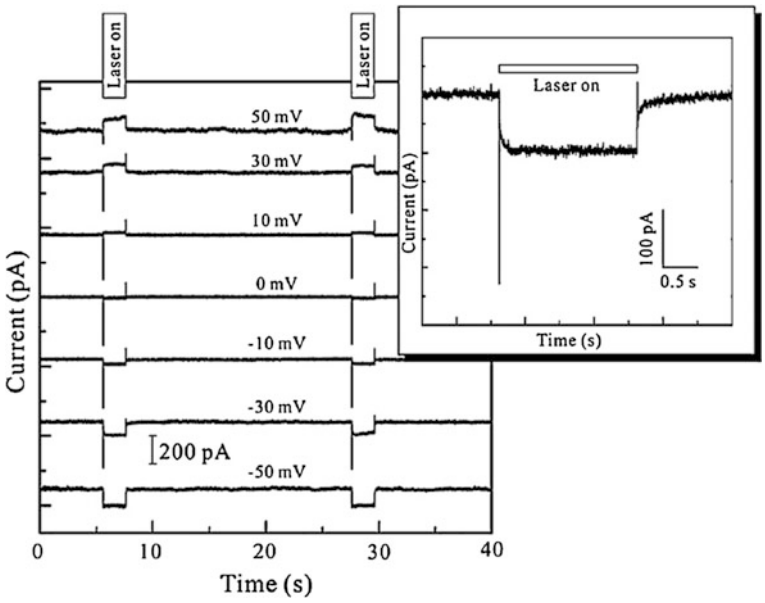

Fig. 4.6 Observed dependence of laser-gated channel current recordings on membrane potential for ChRWR expressing HEK293 cells after 3 days incubation. SOI substrate was used. *Inset* is expanded current profile measured at membrane potential of −30 mV

relaxations are: channelrhodopsin contains a retinal that covalently binds to the apoprotein and the photoisomerization of all-*trans*-retinal to 13-*cis* configuration is coupled to conformational changes in the protein and causes the permeation of ions [17]. Many (∼8) intermediate states including dark states with a lifetime longer than several seconds are observed, and several photocycle models are proposed [17, 28, 31]. The "*on*" transition time to the initial opening state is about 2 ms, and the decay of the photocurrent upon light off strongly depends on the intracellular pH [28]. In the case of the wild-type channelrhodopsin 2 (ChR2), it is excited to the first channel open state by the blue (∼480 nm) light irradiation by the transition time of about 2 ms, and after that it quickly desensitizes to the second channel open state, and then it decays to the dark state by the switching off of the irradiation light with a transition time of about 15 ms [29]. The photocurrent of ChR1 is hardly desensitized during bright light illumination, although that of ChR2 is rapidly desensitized [17, 28]. The *N* terminal segments of ChR2 were replaced with the homologous counterparts of ChR1 and generated several chimeras with different current profiles [17]. In ChRWR, a small desensitization and an almost flat and quite large current profile were realized [17].

In the case of the Si sensor chip, however, the *on* profile was slightly slow (Fig. 4 in Ref. [27]); this may be due to the large capacitance (∼100 pF) of the Si sensor chip compared with the PMMA chip (3–5 pF). Therefore, these data indicate that a current profile with high reliability equivalent to the pipette patch clamp

method can be obtained by using the PMMA sensor chips together with salt-bridge stable electrodes. Without a cell trapping pattern, a long incubation time (>5 days) was necessary to wait for the sensor cell to make stable coverage of the micropore (Fig. 4.4a), and the multiple layers of the sensor cell that were often formed owing to this long incubation time made current measurement impossible. When the cell trapping pattern was present, a single monolayer colony stably covering the micropore was formed in a short incubation time (Fig. 4.4b). Therefore, the cell trapping pattern not only shortened the necessary incubation time (to $\sim$3 days) but also improved the success probability by 10–20 %.

4.3 Ion-Channel Current Recording in Neural Network

4.3.1 Formation of Rat Cerebral Cortex Neuron Network on PC Sensor Chip

Rat embryos of embryonic day 17 were obtained by caesarian section from pregnant mothers, which were anaesthetized with isoflurane (Abbott) and killed by scission of carotid arteries. The use of these animals in the experimental protocols described was approved by the Nagoya University Animal Care Committee. Brains of 8–10 embryos were quickly brought out with surgical scissors, and the cerebral cortex tissue was dissected into small pieces, which were transferred into a 15-ml plastic centrifuge tube with 5 ml Hank's balanced salt solution (HBSS, Gibco) containing 0.25 % trypsin and kept at 37 °C for 20 min in a water bath. HBSS was removed, and neural cells were disassembled by pipetting in 5 ml DMEM with 10 % fetal bovine serum (FBS). The tube was centrifuged at 140*g* for 5 min, and the cell pellet was suspended in 1 ml Neurobasal medium containing B27 (Gibco), 2 mM Glutamax (Gibco), and 5 % FBS. The cells were plated at a density of 1–5 $\times$ 10^4 cells/cm^2 onto an 11 mm square PLL-coated PC sensor chip in 35-mm plastic culture dishes. The cultures were maintained at 37 °C in a humidified atmosphere containing 5 % CO_2 for 10–14 days. After the formation of the neuron network on the PC sensor chip surface, it was set up in the biosensor for the channel current measurements.

4.3.2 Recordings of Spontaneous Ion-Channel Currents in Neural Networks

One of the most important applications of the incubation-type planar patch clamp is the multi-point ion-channel current recordings in neural networks. In this case, the stable electrode is essential since it is more difficult to realize the high-seal resistance due to a very long incubation time. First, we tried to form a neuron network

using a PMMA sensor chip with cell trapping pattern as shown in Fig. 4.1. It was, however, difficult to form a long-term stable neuron network. It was found that the viability of the neuron cells in the cell trapping area was much lower than those outside that area (Fig. 4.7). Stable incubation inside the cell trapping area was observed in PC12 and HEK293 cells. On the other hand, in the case of the primary culture neurons that form a network by making a huge number of synapses, almost all neurons died in our case if they could not form synapses with surrounding neurons within about 1 week. We consider that the cell trapping pattern shown in Fig. 4.1, inside which neurons cannot extend neurites freely, is not suitable for maintaining the neuron network for a long-term culture. Therefore, in this experiment, we seeded rat hippocampal neurons on the PC sensor chip with a flat surface with a density of 1–5 × 10^4 cells/cm^2 and incubated them in the 35-mm dish for 10–14 days. In all sensor chips, inhomogeneous gathering of neurons due to migration was observed, as shown in Fig. 4.8a, and in 1–2 chips out of 10, it was observed that a neural cell existed on the micropore on the chip. The seal resistance was surprisingly small; it was ∼2.7 MΩ before the suction and ∼3.4 MΩ after the suction (n = 5). The sensor chip with a cell on the micropore was set up on the sensor chip position in the ion-channel biosensor shown in Fig. 4.2, and the upper and lower spaces were filled with bath and pipette solutions, respectively. The network formed was already very complex. A large number of multi-synaptic contacts and autaptic contacts [32] were formed. Therefore, we have considered that the measurements of spontaneous channel currents are more important than those of evoked currents induced by artificial stimulation, which makes the network structure much more complex due to synaptic plasticity [33]. Before the nystatin perforation, no channel currents were observed under the voltage clamp, but immediately after the injection of nystatin into the pipette solution, a channel current that depended on the membrane voltage was observed with good

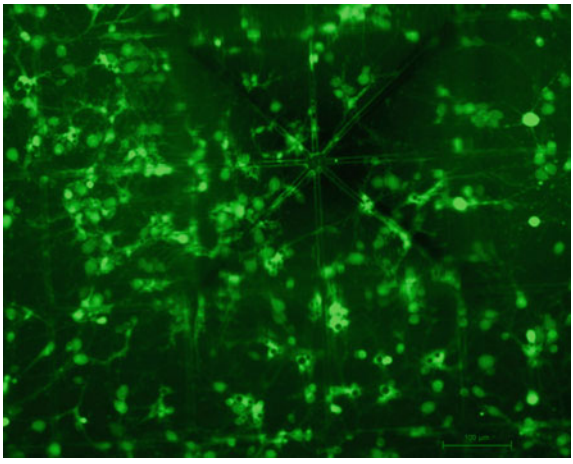

Fig. 4.7 Fluorescence microscopy image of rat cerebral cortex neuron network formed on PMMA substrate after about 2 weeks incubation. Groove pattern is formed and round cell trapping area is formed at crossing point of grooves. The viability of the cell was low inside of the groove or the cell trapping area

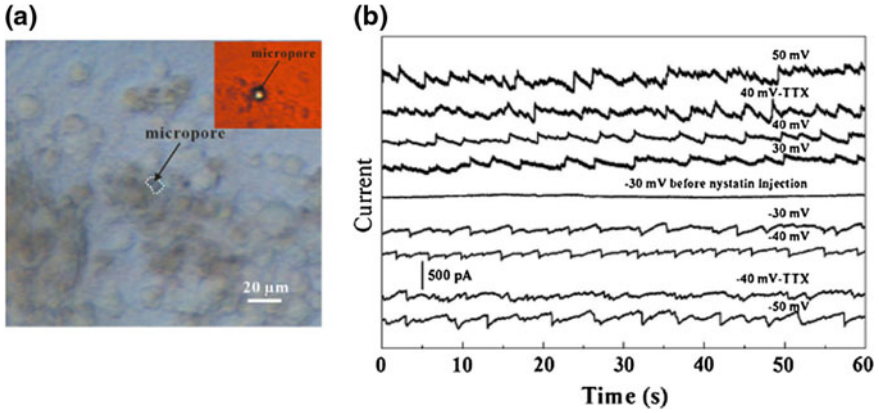

Fig. 4.8 Spontaneous channel current measurements in in vitro neuron network of rat hippocampus. **a** Neuron network of 10 day culture formed on Si-SOI sensor chip with flat surface. **b** Spontaneous channel current observed for various membrane potential value. Effects of TTX addition were investigated for membrane potential at −40 mV and +40 mV. *Smooth line* around centre is recording at membrane potential at −30 mV before nystatin injection to pipette solution. All other recordings were measured after nystatin injection

reproducibility as shown in Fig. 4.8b. It is clear that these signals are due to spontaneous activity of the neural network. By adding tetrodotoxin (TTX), which is a typical antagonist of the Na^+ channel [10, 33]; some unique changes of the channel current profile were observed. At −40 mV, pulse-like current disappeared by adding TTX, but at +40 mV pulse-like current was still observed. Therefore, it is concluded that the observed channel currents are a mixture of many post-synaptic currents evoked by the spontaneous firing of presynaptic neurons and post-synaptic currents induced by the spontaneous neurotransmitter emission, which are called miniature excitatory post-synaptic currents (mEPSC) and miniature inhibitory post-synaptic currents (mIPSC) [33]. It is entirely due to the stable electrodes that the spontaneous channel currents were successfully observed. Since inhomogeneous gathering of neurons due to migration makes meaningful multi-point measurements impossible, we are now developing a new type of cell trapping pattern and cell seeding technique that hinders cell migration and enables the formation of more homogeneous neural networks.

4.4 Future Prospects and Disease Model Chip

For neurodegenerative diseases, such as ALS and AD, many mutated genes that cause the onset of the disease have already been discovered. Therefore, considering that neurodegenerative diseases such as ALS and AD are unique to humans, the in vitro neural network containing mutated genes is considered to be the most useful

disease model, which can be used for developing new drugs that are effective in treating the diseases. We can make the disease model by making the neuron network from human iPS cells and transfecting the mutated genes. In this case, however, this disease model has a limitation; it cannot be used to investigate the cause of diseases, that is, to investigate how the mutations are introduced.

As already mentioned, neurons easily aggregate due to the nature of migrations, especially in the case of high density cultures, which are close to the real brain neuron network, and spontaneous firing is observed with a frequency of about 2–3/s in frequent cases [34]. Therefore, it is necessary to develop a technology to form an in vitro neuron network without inhomogeneous aggregations. Furthermore, the soma of the neuron must be set on the micropore of the substrate, in the case of the planar patch clamp. As the first step to the realization of a disease model, we have developed the substrate for an incubation-type planar patch clamp suitable for long term incubation of a neuron network (Fig. 4.9). The cell trapping area is surrounded by several pillars that are 30 μm in diameter and about 8 μm in height, by which cell migration is limited, but axon and dendrites can extend through the gap between the pillars. Micropores with a diameter of about 2 μm for the ion-channel current measurements are formed inside the several cell trapping area. The network of the rat cerebral cortex neuron formed by seeding the cells selectively inside the cell trapping area is shown in Fig. 4.9b. In the near future, we are going to form complex neuron networks on this substrate consisting of several kinds of brain cells such as motor neurons, cerebral cortex neurons, and glia cells formed from human iPS cells by differentiation.

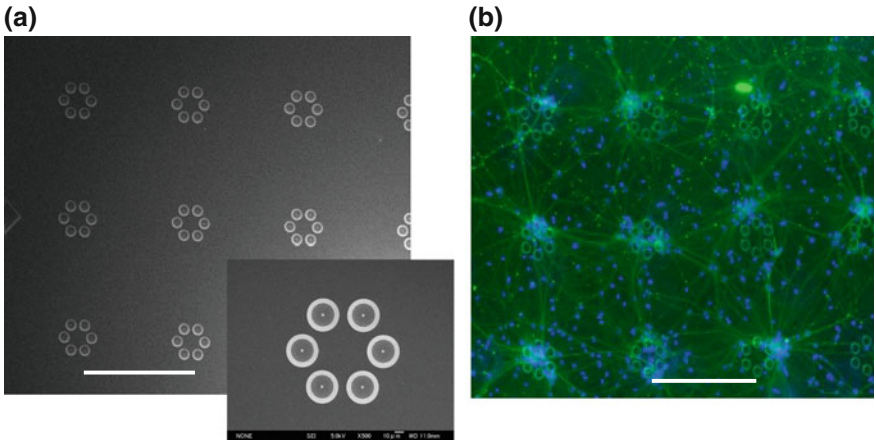

Fig. 4.9 **a** Scanning microscopy image of PC substrate developed for homogeneous neuron network formation. Many cell trapping areas surrounded by six pillars are observed. Diameter and height are ∼30 and ∼8 μm, respectively. Gap between neighbouring pillars is ∼9 μm. **b** Fluorescence microscopy image of rat cerebral cortex neuron network after 13 day incubation. Cells were seeded on cell trapping pattern area selectively. *Green* and *blue* are tubulin and DAPI staining, respectively. *Scale bar* is 300 μm

4.5 Summary

Optogenetic tools, such as channelrhodopsin and halorhodopsin, are useful to investigate the function of neuron networks due to their high spatial and temporal resolutions. In this chapter, however, another application of channelrhodopsin is introduced. We are developing a high-throughput screening device, which is necessary for investigation of the cause and new drag development of neurodegenerative diseases. Since ion-channel current measurement is considered to give the most important information to analyze the neuron network functions, we have developed a planar patch clamp device with incubation function using ChRWR for the performance test of the device. In the development, the large noise due to the low-seal resistance of the incubation-type planar patch clamp was significantly reduced, and we succeeded in taking ion-channel current measurements in the in vitro neuron network of rat cerebral cortex for the first time. We are now developing a disease model of a neurodegenerative disease, such as ALS and/or AD based on the in vitro neuron network formed from human iPS cells. We believe that a new important way to elucidate the cause and development of the treatment method of these intractable diseases can be found by combining these disease models of neuron networks and the high-throughput screening device.

Acknowledgments The authors thank the staff of the Equipment Development Centre of the Institute for Molecular Science, especially Ms. Noriko Takada, Mr. Masaki Aoyama, and Mitsukazu Suzui, for their support with device fabrication. The authors also thank the group leaders of the CREST team, Profs. Yugo Fukazawa, Toru Ishizuka, Yuji Furutani, Tetsunari Kimura, and Yuki Sudo, for their support with channelrhodopsin and meaningful discussions.

References

1. T. Urisu, T. Asano, Z. Zhang, H. Uno, R. Tero, H. Junkyu, I. Hiroko, Y. Arima, H. Iwata, K. Shibasaki, M. Tominaga, Incubation type Si-based planar ion channel biosensor. Anal. Bioanal. Chem. **391**, 2703–2709 (2008)
2. H. Uno, Z.-H. Wang, Y. Nagaoka, N. Takada, S. Obuliraj, K. Kobayashi, T. Ishizuka, H. Yawo, Y. Komatsu, T. Urisu, Improvement of performances in incubation-type planar patch clamp biosensor by using salt bridge electrode and plastic (PMMA) substrates. Sens. Actuators, B Chem. **193**, 660–668 (2014)
3. N. Fertig, R.H. Blick, J.C. Behrends, Whole cell patch clamp recording performed on a planar glass chip. Biophys. J. **82**, 3056–3062 (2002)
4. T. Sordel, F. Kermarrec, Y. Sinquin, I. Fonteille, M. Labeau, F. Sauter-Starace, C. Pudda, F. de Crécy, F. Chatelain, M. De Waard, C. Arnoult, N. Picollet-D'hahan, The development of high quality seals for silicon patch-clamp chips. Biomaterials **31**, 7398–7410 (2010)
5. B. Matthews, J.W. Judy, Design and fabrication of a micromachined planar patch-clamp substrate with integrated microfluidics for single-cell measurements. J. Microelectromech. Syst. **15**, 214–222 (2006)
6. R. Pantoja, J.M. Nagarah, D.M. Starace, N.A. Melosh, R. Blunck, F. Bezanilla, J.R. Heath, Silicon chip-based patch-clamp electrodes integrated with PDMS microfluidics. Biosens. Bioelectron. **20**, 509–517 (2004)

7. A. Stett, C. Burkhardt, U. Weber, P.V. Stiphout, T. Knott, CYTOCENTERING: a novel technique enabling automated cell-by-cell patch clamping with the CYTOPATCH chip. Recept. Channels **9**, 59–66 (2003)
8. X. Li, K.G. Klemic, M.A. Reed, F.J. Sigworth, Microfluidic system for planar patchclamp electrode arrays. Nano Lett. **6**, 815–819 (2006)
9. H. Uno, Z.-L. Zhang, K. Suzui, R. Tero, Y. Nonogaki, S. Nakao, S. Seki, S. Tagawa, S. Oiki, T. Urisu, Noise analysis of Si-based planar-type ion-channel biosensors. Jpn. J. Appl. Phys. **45**, L1334–L1336 (2006)
10. H.-Z.W. Tao, L.I. Zhang, G.-Q. Bi, M.-M. Poo, Selective presynaptic propagation of long-term potentiation in defined neural networks. J. Neurosci. **20**, 3233–3243 (2000)
11. A.M. Taylor, D.C. Dieterich, H.T. Ito, S.A. Kim, E.M. Schuman, Microfluidic local perfusion chambers for the visualization and manipulation of synapses. Neuron **66**, 57–68 (2010)
12. A. Reska, P. Gasteier, P. Schulte, M. Moeller, A. Offenhäusser, J. Groll, Ultrathin coatings with change in reactivity over time enable functional in vitro networks of insect neurons. Adv. Mater. **20**, 2751–2755 (2008)
13. J. Erickson, A. Tooker, Y.C. Tai, J. Pine, Caged neuron MEA: a system for long-term investigation of cultured neuronal network connectivity. J. Neurosci. Methods **175**, 1–16 (2008)
14. T. Asano, H. Uno, K. Shibasaki, M. Tominaga, T. Urisu, A cell culture type planar ion-channel biosensor. Trans. Mater. Res. Soc. **33**, 767–770 (2008)
15. F. Zhang, L.-P. Wang, E.S. Boyden, K. Deisseroth, Channelrhodopsin-2 and optical control of excitable cells. Nat. Methods **3**, 785–792 (2006)
16. L. Petreanu, D. Huber, A. Sobczyk, K. Svoboda, Channelrhodopsin-2-assisted circuit mapping of long-range callosal projections. Nat. Neurosci. **10**, 663–668 (2007)
17. H.Y. Wang, Y. Sugiyama, H. Hikima, E. Sugano, H. Tomita, T. Takahashi, T. Ishizuka, H. Yawo, Molecular determinants differentiating photocurrent properties of two channelrhodopsins from chlamydomonas. J. Biol. Chem. **284**, 5685–5696 (2009)
18. N. Takada, M. Aoyama, M. Suzui, Y. Hachisu, H. Ohmori, Z.-H. Wang, S. Obuliraju, Y. Nagaoka, M. Goto-Saitoh, T. Urisu, Microfabrication of PMMA sensor chips for an incubation type planar patch clamp. Int. J. Nanomanuf. **10**, 281–294 (2014)
19. A. Rekas, J.R. Alattia, T. Nagai, A. Miyawaki, M. Ikura, Crystal structure of Venus, a yellow fluorescent protein with improved maturation and reduced environmental sensitivity. J. Biol. Chem. **277**, 50573–50578 (2002)
20. T. Nagai, K. Ibata, E.S. Park, M. Kubota, K. Mikoshiba, A. Miyawaki, A variant of yellow fluorescent protein with fast and efficient maturation for cell-biological applications. Nat. Biotechnol. **20**, 87–90 (2002)
21. M.J. Caterina, M.A. Schumacher, M. Tominaga, T.A. Rosen, J.D. Levine, D. Julius, The capsaicin receptor: a heat-activated ion channel in the pain pathway. Nature **389**, 816–824 (1997)
22. N. Akaike, N. Harata, Nystatin perforated-patch recording and its applications to analyses of intracellular mechanisms. Jpn. J. Physiol. **44**, 433–473 (1994)
23. L. Vyklický, K. Nováková-Toŭsová, J. Benedikt, A. Samad, F. Toŭska, V. Vlachová, Calcium-dependent desensitization of vanilloid receptor TRPV1: a mechanismpossibly involved in analgesia induced by topical application of capsaicin. Physiol. Res. **57**, S59–S68 (2008)
24. E.A. Schwartz, Depolarization without calcium can release gamma-aminobutyric acid from a retinal neuron. Science **238**, 350–355 (1987)
25. Y. Kataoka, H. Ohmori, Activation of glutamate receptors in response to mem-brane depolarization of hair cells isolated from chick cochlea. J. Physiol. **477**, 403–414 (1994)
26. A. Hazama, S. Hayashi, Y. Okada, Cell surface measurements of ATP release fromsingle pancreatic beta cells using a novel biosensor technique. Pflug. Arch. **437**, 31–35 (1998)
27. Z.-H. Wang, N. Takada, H. Uno, T. Ishizuka, H. Yawo, T. Urisu, Positioning of the sensor cell on the sensing area using cell trapping pattern in incubation type planar patch clamp biosensor. Colloids Surf., B **96**, 44–49 (2012)

28. G. Nagel, T. Szellas, W. Huhn, S. Kateriya, N. Adeishvili, P. Berthold, D. Ollig, P. Hegeman, E. Bamberg, Channelrhodopsin-2 a directly light-gated cation-selective membrane channel. Proc. Natl. Acad. Sci. USA **100**, 13940–13945 (2003)
29. T. Ishizuka, M. Kakuda, R. Araki, H. Yawo, Kinetic evaluation of photosensitivity in genetically engineered neurons expressing green algae light-gated channels. Neurosci. Res. **54**, 85–94 (2006)
30. C. Bamann, T. Kirsch, G. Nagel, E. Bamberg, Spectral characteristics of the pho-tocycle of channelrhodopsin-2 and its implication for channel function. J. Mol. Biol. **375**, 686–694 (2008)
31. K. Stehfest, P. Hegemann, Evolution of the channelrhodopsin photocycle model. ChemPhysChem **11**, 1120–1126 (2010)
32. B.R. Rost, J. Breustedt, A. Schoenherr, G. Grosse, G. Ahnert-Hilger, D. Schmitz, Autaptic cultures of single hippocampal granule cells of mice and rats. Eur. J. Neurosci. **32**, 939–947 (2010)
33. K.S. Wilcox, J. Buchhalter, M.A. Dichter, Properties of inhibitory and excitatory synapses between hippocampal neurons in very low density cultures. Synapses **18**, 128–151 (1994)
34. B.-Q. Mao, F. Hamzei-Sichani, D. Aronov, R. C. Froemke, R. Yuste, Dynamics of Spontaneous Activity in Neocortical Slices. Neuron **32**, 883–898 (2001)